https://doi.org/10.5194/amt-2019-324
Preprint. Discussion started: 18 December 2019

Atmospheric Measurement Techniques Discussions

Separation of Convective and Stratiform Precipitation Using Polarimetric Radar Data with A Support Vector Machine Method

Yadong Wang[1], Lin Tang[2], Pao-Liang Chang[3], and Yu-Shuang Tang[3]

[1]Electrical and Computer Engineering Department, Southern Illinois University Edwardsville, Illinois, USA
[2]Cooperative Institute for Mesoscale Meteorological Studies, University of Oklahoma, NOAA/OAR/National Severe Storms Laboratory, Norman, Oklahoma, USA
[3]Central Weather Bureau, Taipei, Taiwan

Correspondence: Yadong Wang (yadwang@siue.edu)

Abstract. A precipitation separation approach using a support vector machine method was developed and tested on a C-band polarimetric weather radar located in Taiwan (RCMK). Different from some existing methods requiring a whole volume scan data, the proposed approach utilizes the polarimetric radar data from the lowest tilt to classify precipitation echoes into either stratiform or convective type. Through a support vector machine method, the inputs of radar reflectivity, differential reflectivity, and the separation index are integrated in the classification. The feature vector and weight vector in the support vector machine were optimized using well-classified training data. The proposed approach was tested with multiple precipitation events including two widespread mixed stratiform and convective events, a tropical typhoon precipitation event, and a stratiform precipitation event. In the evaluation, the results from the multi-radar-multi-sensor (MRMS) precipitation classification approach were used as the ground truth, and the performances from proposed approach were further compared with the approach using separation index only with different thresholds. It was found that the proposed method can accurately identify the convective cells from stratiform rain, and produce better results than using the separation index only.

1 Introduction

Convective and stratiform precipitations exhibit significant differences in precipitation growth mechanisms and thermodynamic structures (e.g., Houghton, 1968; Houze, 1993, 1997). Generally, convective precipitation is associated with strong but small areal vertical air motion (> 5 m s^{-1}) (Penide et al., 2013), and delivers high rainfall rate (R) (Anagnostou, 2004). On the other hand, stratiform precipitation is associated with weak updrafts/downdrafts (< 3 m s^{-1}) and relative low R. Therefore, classifying a precipitation into either convective or stratiform type not only promotes the understanding of cloud physics, but also enhances the accuracy of quantitative precipitation estimation (QPE). For these purposes, numerous methods using ground in situ measurements or satellite observations were developed during the past four decades (e.g., Leary and Jr., 1979; Adler and Negri, 1988; Tokay and Short, 1996; Hong et al., 1999).

Ground-based weather radars, such as Weather Surveillance Radar, 1988, Doppler (WSR-88D), are currently used in all aspects of weather diagnosis and analysis. Precipitation classification using single- or dual-polarization radars were developed during the past three decades. For a single-polarization radar, developed algorithms mainly rely on radar reflectivity (Z) and

https://doi.org/10.5194/amt-2019-324
Preprint. Discussion started: 18 December 2019

Atmospheric Measurement Techniques Discussions

its derived variables (e.g., Biggerstaff and Listemaa, 2000; Anagnostou, 2004; Yang et al., 2013; Powell et al., 2016). For example, Steiner et al. (1995) (hereafter SHY95) proposed a separation approach that utilizes the texture features derived from radar reflectivity field. In this approach, a grid point in Z field is identified as the convective center if its value is larger than 40 dBZ, or exceeds the average intensity taken over the surrounding background by specified thresholds. Those grid points surrounding the convective centers are classified as convective area, and far regions are classified as stratiform. Penide et al. (2013) found that SHY95 may misclassify those isolated points embedded within stratiform precipitation or associated with low cloud-top height. Powell et al. (2016) modified SHY95′s approach, and the new approach can identify shallow convection embedded within large stratiform regions, and those isolated shallow and weak convections. A neural network based convective-stratiform classification algorithm was developed by Anagnostou (2004). It utilizes six variables as inputs including storm height, reflectivity at 2 km elevation, vertical gradient of reflectivity, the difference in height, the standard deviation of reflectivity, and the product of reflectivity and height. Similar variables are also used in a fuzzy logic based classification approach proposed by Yang et al. (2013).

Although these listed classification algorithms have been developed and validated for years, a robust algorithm utilizing the lowest tilt radar data only is still needed for the following two reasons. First, according to U.S. Radar Operations Center (ROC), the WSR-88D radars are currently operated without updating a complete volume during each volume scan, especially during precipitation events. New radar scanning schemes are designed to reorganize the updating order for a high frequency in low elevations and a less frequency for high elevations. Therefore, WSR-88D radars are able to promptly capture the storm development for weather forecast and to obtain a more accurate precipitation estimation. These new schemes include the automated volume scan evaluation and termination (AVSET), supplemental adaptive intra-volume low-level scan (SAILS), the multiple elevation scan option for SAILS, and the mid-volume rescan of low-level elevations (MRLE). Under these new scanning schemes, the separation of stratiform/convective becomes challenge for those algorithms requiring a full volume scan of data. Second, with the developments in radar polarimetry, polarimetric weather radars have been well applied in radar QPE, severe weather detection, hydrometeor classification, and microphysical retrievals (Ryzhkov and Zrnic, 2019; Zhang, 2016). Through transmitting and receiving electromagnetic waves along the horizontal and vertical directions, a polarimetric radar can obtain extra information about hydrometeors' size, shape, species, and orientation. Therefore, the polarimetric measurements may reveal more precipitation's microphysical and dynamic properties. Inspired by these features, a C-band polarimetric radar precipitation separation approach was developed by Bringi et al. (2009) (hereafter BAL), which classifies the precipitation into stratiform, convective and transition regions based on retrieved drop size distribution (DSD) characteristics. However, it was found that strong stratiform echoes might have similar DSDs to weak convective echoes and lead to wrong classification results (Powell et al., 2016).

In this work, a novel precipitation separation algorithm using separation index with other radar variables was developed and tested on a C-band polarimetric radar located in Taiwan. This approach classifies precipitations into stratiform or convective type with a support vector machine (SVM) method. Different from some existing classification techniques that require the whole volume scan of radar data, this new approach uses the unblocked data from the lowest scanning tilt. The major advantage of this method is that it can provide real-time classification results even if the radar is operated under AVSET, SAILS, and

https://doi.org/10.5194/amt-2019-324
Preprint. Discussion started: 18 December 2019

Atmospheric Measurement Techniques Discussions

MRLE scanning schemes, where the lowest tilt is the most frequently scanned and updated. This paper is organized as follows: section 2 introduces the proposed method including radar variables and processings, the SVM method, and the training process. The performance evaluation is shown in Section 3, and the discussion and summary are given in Section 4.

2 Precipitation Separation With a Support Vector Machine Method

In the current work, the SVM precipitation separation approach was developed and validated on a C-band polarimetric radar (RCMK) located at Makung, Taiwan (Figure 1). The Weather Wing of the Chinese Air Force deployed this radar and made the data available to the Central Weather Bureau (CWB) of Taiwan since 2009. Together with three single-polarization S-band WSR-88D (RCCG, RCKT, and RCHL) and one dual-polarization S-band radar (RCWF), these five radars provide real-time QPEs for CWB to support missions of flood monitoring and prediction, landslide forecasts and water resource management.

2.1 Input polarimetric radar variables and preprocesses

Three direct measured or derived radar variables are proposed as inputs to the SVM approach: Z, differential reflectivity fields (Z_{DR}), and separation index (i). In most of precipitation classification approaches, Z is used as one of inputs because reflectivities from convective generally show higher values than from stratiform type. For example, a radar echo with the reflectivity of 40 dBZ and above is automatically classified as convective type in the approach developed by SHY95.

Differential reflectivity, which is highly related to raindrop's mass weighted mean diameter (D_m), is another good indicator of precipitation type. It was found the values of D_m in stratiform and convective precipitation generally are within 1-1.9 mm and above 1.9 mm, respectively (Chang et al., 2009). Higher Z_{DR} values are expected from convective than stratiform precipitation. Therefore, Z_{DR} field is used as another input of the proposed approach.

For short wavelength radars such as C-band or X-band radars, the Z and Z_{DR} fields may be significantly attenuated when the radar beam propagates through heavy precipitation regions. Both Z and Z_{DR} fields need to be corrected from attenuation before applied in the precipitation classification and QPE. Different attenuation correction methods were proposed using the differential phase (ϕ_{DP}) measurement such as the linear ϕ_{DP} approach, the standard ZPHI method, and the iterative ZPHI method (e.g., Jameson, 1992; Carey et al., 2000; Testud et al., 2000; Park et al., 2005). Because of its simplicity and easy implementation in a real-time system, the linear ϕ_{DP} method was applied in the current work.

$$Z(r) = Z'(r) + \alpha(\phi_{DP}(r) - \phi_{DP}(0)) \tag{1a}$$

$$Z_{DR}(r) = Z'_{DR}(r) + \beta(\phi_{DP}(r) - \phi_{DP}(0)) \tag{1b}$$

where $Z'(r)$ ($Z'_{DR}(r)$) is the observed reflectivity (differential reflectivity) at range r; $Z(r)$ ($Z_{DR}(r)$) is the corrected value; $\phi_{DP}(0)$ is the system value; $\phi_{DP}(r)$ is the smoothed (by FIR filter) differential phase at range r. The attenuation correction coefficients α and β depend on DSD, drop size shape relations (DSR), and temperature. The typical range of α (β) is found 0.06∼0.15 (0.01∼0.03) dB deg^{-1} for C-band radars (e.g., Carey et al., 2000; Vulpiani et al., 2012). Following the work from

https://doi.org/10.5194/amt-2019-324
Preprint. Discussion started: 18 December 2019

Atmospheric Measurement Techniques Discussions

Wang et al. (2014), optimal coefficients α and β in Taiwan are 0.088 dB deg^{-1} and 0.02 dB deg^{-1}, respectively. The Z and Z_{DR} fields are further smoothed with a 3 (azimuthal) by 3 (range) moving window function after corrected from attenuation.

Using the separation index i to identify convective from stratiform precipitation was originally proposed by BAL, where i was calculated under a normalized gamma DSD assumption:

$$i = log_{10}(N_W^{est}) - log_{10}(N_W^{sep}) \tag{2}$$

$$log_{10}(N_W^{sep}) = -1.6D_0 + 6.3 \tag{3}$$

where N_W^{est} is the estimated N_W (normalized number concentration) from observed Z and Z_{DR}, and is calculated as:

$$N_W^{est} = Z/0.056D_0^{7.319} \tag{4}$$

In Equation 4, D_0 is the median volume diameter, and can be calculated as.

$$D_0 = 0.0203Z_{DR}^4 - 0.1488Z_{DR}^3 + 0.2209Z_{DR}^2 + 0.5571Z_{DR} + 0.801; \quad -0.5 \le Z_{DR} < 1.25 \tag{5a}$$

$$= -0.0355Z_{DR}^3 - 0.3021Z_{DR}^2 + 1.0556Z_{DR} + 0.6844; \quad 1.25 \le Z_{DR} < 5 \tag{5b}$$

The units of Z_{DR}, Z, N_w, and D_0 are dB, mm^{6}m^{-3}, mm^{-1}m^{-3}, and mm, respectively. The positive and negative values of index i indicate convective and stratiform rain, respectively, and $|i| < 0.1$ indicates transition regions (Penide et al., 2013). BAL pointed out that index i worked well in most of the cases in their study; however, incorrect classification results are likely obtained for low Z and high Z_{DR} cases in some convective precipitations.

2.2 Drop size distribution and drop shape relation

It should be noted that the relations between Z, N_w, and D_0 were derived using the DSD data collected in Darwin, Australia. Coefficients in Equations 2∼5 need be adjusted according to different frequency radars or/and other DSD and DSR features from the specific location (Thompson et al., 2015). In the current work, the separation index i derived using Equations 2∼5 is directly used as one of the input variables. It was shown by Wang et al. (2013) that DSD and DSR features in Taiwan is very similar to those measured from Darwin, Australia. Similar $R(K_{DP})$ relationships were obtained using data collected from these two locations. Coefficients derived by BAL could be directly used in Taiwan without further modification. To verify this assumption, N_w and D_0 were calculated using DSD data collected by four impact-type Joss-Waldvogel disdrometers (JWD) located in Taiwan (Figure 1). The measurement range and temporal resolution of these JWDs are 0.359 mm ∼ 5.373 mm and 1 minute, respectively. Total 4306-minute data from 2011∼2014 are used in N_w and D_0 calculation following the approach described in Bringi et al. (2003). Similar to the work presented in BAL, the distribution of i along median volume diameter D_0 is shown in Figure 2, where the ($log_{10}N_w$, D_0) pairs from stratiform and convective types are represented with gray circles and black stars, respectively. Although the relation described in Equation 3 can separate most stratiform from convective types, a large number of points are still classified incorrectly. Therefore, the single separation index is not sufficient in the precipitation separation, and other variables such as Z and Z_{DR} may be used as the supplement.

https://doi.org/10.5194/amt-2019-324
Preprint. Discussion started: 18 December 2019

Atmospheric Measurement Techniques Discussions

2.3 Support vector machines (SVM) method

2.3.1 Introduction of SVM

Support vector machine (SVM) can be viewed as a kernel-based machine learning approach, which nonlinearly maps the data from the low-dimension input space to a high-dimension feature space, and then linearly maps to a binary output space (Burges, 1998). Given a set of training samples, the SVM constructs an optimal hyperplane, which maximizes the margin of separation between positive and negative examples (Haykin, 2011). Specifically, given a set of training data $\{(X_i, y_i)\}_{i=1}^{N}$, the goal is to find the optimal weights vector W and a bias b such that

$$y_i(W^T X_i + b) \geq 1 \qquad i = 1, 2, ..., N \tag{6}$$

where $X_i \in \mathbb{R}^m$ is the input vector, m is the input variable dimension (m = 3 in this work), N is the number of training samples, and y_i is an output with the value of $+1$ or -1 that represents convective or stratiform, respectively. The particular data points (X_i, y_i) are called support vector when Equation 6 is satisfied with the equality sign. The optimum weights vector W and bias b can be obtained through solving the Lagrangian function with the minimum cost function (Haykin, 2011).

Since the SVM can be viewed as a kernel machine, finding the optimal weight vector and bias in Equation 6 can be alternatively solved through the recursive least square estimations of:

$$\sum_{i=1}^{N_s} \alpha_i y_i k(X, X_i) = 0 \tag{7}$$

where N_s is the number of support vectors, α_i is the Lagrange multipliers, and $k(X, X_i)$ is the Mercer kernel defined as:

$$k(X, X_i) = \Phi^T(X_i)\Phi(X) = exp\left(-\frac{1}{2\sigma^2}||X - X_i||^2\right) \tag{8}$$

With the solved $\{\alpha_i\}_{i=1}^{N}$, the SVM calculate the classification results with new input data $Z \in \mathbb{R}^m$ as:

$$f(Z) = sign[\left[\sum_{i=1}^{N_s} \alpha_i y_i \Phi^T(X_i)\Phi(Z)\right] \tag{9}$$

When $f(Z) = 1$, the output is classified as convective, otherwise is classified as stratiform.

2.3.2 Training of the SVM

In the SVM approach, the weight vector and bias in Equation 6 need to be optimized through a recursive least square estimation using the training data set. Since the training data play a critical role in the SVM approach, Z, Z_{DR} and i from convective and stratiform precipitation events were carefully examined through three steps. Firstly, the training data was checked following general classification principles. For example, training data from convective precipitation is generally associated with relative strong reflectivity, no apparent bight band signature, and high vertically integrated liquid (VIL). Secondly, the precipitation type is verified by ground observation such as ground severe storm report. Thirdly, the precipitation type is confirmed by the

https://doi.org/10.5194/amt-2019-324
Preprint. Discussion started: 18 December 2019

Atmospheric Measurement Techniques Discussions

Multi-Radar-Multi-Sensor (MRMS) precipitation classification algorithm implemented in Taiwan (Zhang et al., 2011, 2016). In this MRMS classification approach, a 3-dimensional radar reflectivity field was mosaicked from 4 S-band single polarization radars (Figure 1), and the composite reflectivity (CREF) together with other fields such as temperature and moisture fields were then used in the surface precipitation classification (Zhang et al., 2016). Based on the classification results, MRMS chooses different $R(Z)$ relations in the rainfall rate estimation. The performance of MRMS has been thoroughly evaluated for years for the quantitative precipitation estimation, flash flood monitoring, severe weather and aviation weather surveillance (e.g., Gourley et al., 2016; Smith et al., 2016), and also used as the benchmark and/or ground truth in many studies (e.g., Grecu et al., 2016; Skofronick-Jackson and Coauthors, 2017). It should be noted that, although the performance of MRMS is well accepted in weather research community, there may be some imperfections in this system, especially it only uses single-polarization variables to determine the precipitation type. Other observations, such as the accumulated rainfall amount measured by gauges may be another reference. However, biases in the gauge measurements and improper $R(Z)$ relations may causes other uncertainties. Therefore, at the current stage, MRMS precipitation classification result is the best benchmark in the training and validation of the proposed algorithm. Moreover, since the MRMS classification results are derived from 4 S-band radars, it can be viewed as an independent reference.

Training data for convective type are mainly from a strong convective precipitation event on 23 July 2014. This thunderstorm, classified as convective precipitation by MRMS, was associated with strong updrafts/downdrafts and caused an aircraft crash on the airport of Makung at 1106 UTC. Radar data collected from 1030 to 1130 UTC were used as the convective type training data. Moreover, the training data are selected when they are associated with $Z > 20$ dBZ, and correlation coefficient $(\rho_{HV}) > 0.98$. The stratiform type data are from a mixed stratiform and convective precipitation even on 30 August 2011, and only those data identified as a stratiform type by MRMS are used in training. Total 17281 sets of data (15144 sets of stratiform, and 2137 sets of convective) are used in the training process. The number of support vectors is selected as 1000 in the current work, and the training process is considered as completed when the root-mean-square error reaches a stable value. In the SVM approach, the original 3-dimension input space is nonlinearly maps to a 1000-dimension feature space, and then linearly maps to a binary output space (Burges, 1998). The higher dimension feature space potentially capture more input variables feature, but higher computation cost is needed. Generally, after the number of support vector reach some number, the enhancement in the performance the SVM approach becomes slight. There is a balance between accuracy and computation. In the current work, the numbers of support vectors were tested at 500, 750, 1000, 2000, and 5000, and 1000 can produce less than 5% error with reasonable computation time. As the prototype algorithm, the number of support vectors is selected as 1000 in the current work.

3 Performance Evaluation

3.1 Description of the experiments

The performance of the proposed approach was validated with four precipitation events from 2009 to 2012. These four precipitation events include one stratiform event, one strong tropical precipitation event, and two events of the mixed convective and

https://doi.org/10.5194/amt-2019-324
Preprint. Discussion started: 18 December 2019


Atmospheric Measurement Techniques Discussions

stratiform. Two experiments based on the BAL approach with different thresholds (i.e., BAL^0 and $BAL^{-0.5}$) were also carried out in the evaluation. In these two experiments, the separation index i from each radar gate is first calculated using Equations 2∼5, and thresholds of T_0 = 0 and -0.5 are then used to separate convective type from stratiform type. A pixel is classified as convective if i is larger than T_0, and as stratiform otherwise. This work aims at developing a complementary method using separation index i together with other variables to separate convective from stratiform type. The proposed SVM and BAL methods both can classify the precipitation using the lowest tilt radar data only, which is suitable for fast scanning and quick updated purpose. Other classification approaches as introduced in section 1 were not examined in the current work, because they require the data from multiple elevation angles.

The MRMS classification products are used as the reference "ground truth" in the evaluation. Because the MRMS results are derived using the mosaicked field from four S-band single-polarization radars, the coverage and time stamp are different from the result of the single radar RCMK. The classification results from RCMK (i.e., BAL^0 , $BAL^{-0.5}$ and SVM) and MRMS could be significantly different with timestamp difference as large as 5 minutes. Given the fact that the convective storms size, intensity, and cells locations could change significantly during a 5-minute period, it is not appropriate to quantitatively evaluate the performance using the pixel-to-pixel evaluation criteria of the probability of detection (POD) and false alarm rate (FAR). Qualitative evaluation maybe the best option for this work, which include two major steps: 1.) Since the MRMS output has much bigger coverage, the MRMS is first truncated according to the coverage of RCMK. This step can assure the RCMK and MRMS have the same precipitation grids. 2.) A whole coverage convective ratio (R^{CS}) is introduced as:

$$R^{CS} = \frac{N^{con}}{N^{con} + N^{str}} \times 100\% \tag{10}$$

Where N^{con} and N^{str} are the total pixel numbers of convective and stratiform types within the coverage, respectively. The evaluation results are shown in the following sections, and the overall performances of R^{CS} from the evaluation cases are presented in Table 1.

3.2 Experiment results

3.2.1 Widespread mixed stratiform and convective precipitations

The performance of the proposed approach was first validated with two widespread stratiform and convective mixed precipitation events from 30 August 2011 and 14 June 2012. For these two cases, 24-hour data (0000 UTC∼2400 UTC) were used in the evaluation. The results from the BAL approach (BAL^0 and $BAL^{-0.5}$) were also calculated. It should be noted that the threshold of -0.5 is lower than the value suggested by BAL, and more pixels will be classified as convective by $BAL^{-0.5}$. The classification results from the proposed SVM were calculated using the trained weight vector and biases, and the convective ratios from MRMS, SVM, BAL^0, and $BAL^{-0.5}$ were calculated using Equation 10.

The time series plots of R^{CS} are shown in Figure 3, where results from 30 August 2011 and 14 June 2012 are shown on panel "a" and "b", and the R^{CS} from MRMS, SVM, BAL^0, and $BAL^{-0.5}$ are presented by thick solid, thick dashed, thin solid and thin dashed lines, respectively. In general, $BAL^{-0.5}$ classifies more pixels as convective than BAL^0 as expected for

https://doi.org/10.5194/amt-2019-324
Preprint. Discussion started: 18 December 2019

Atmospheric Measurement Techniques Discussions

both cases, and SVM shows the most similar results to MRMS comparing to BAL approaches. For the 30 August 2011 case (Figure 3a), if the MRMS results are considered as the ground truth, BAL^0 shows obvious under classification of convective type during this 24-hour period, but BAL$^{-0.5}$ shows better performance. On the other hand, BAL$^{-0.5}$ classifies more pixels as a convective type than MRMS in the 14 June 2012 case (Figure 3b), but the results from BAL^0 are more consistent with MRMS outputs. The overall R^{CS} from MRMS, SVM, BAL^0, and BAL$^{-0.5}$ are shown in Table 1.

To better understand the performance of each approach, the classification results and radar variables (Z, Z_{DR}, and i) from two distinct moments were examined and shown in Figures 4∼7. Classification results from 0303 UTC 30 August 2011 were first shown in Figure 4, where BAL^0, BAL$^{-0.5}$, SVM and MRMS are shown in panel 'a', 'b', 'c', and 'd', respectively. The time stamp for MRMS result is 0300 UTC and the time difference from the other three approaches is about 3 minutes. These three input variables of SVM at 0303 UTC are shown in Figure 5, where Z, Z_{DR}, and i are presented in panel 'a', 'b', and 'c'. From Figures 3 and 4, it could be found that the R^{CS} from MRMS, SVM, and BAL$^{-0.5}$ show similar value, but R^{CS} from BAL^0 is obviously low. Within the black circle of Figure 5, the averages of Z and Z_{DR} both show relatively large values (Z > 36 dBZ and Z_{DR} > 0.75 dB), this is a clear indication of convective type precipitation. Both SVM and BAL$^{-0.5}$ classify most of the area within the black circle as convective, and this result is consistent with the MRMS result. Since the separation indexes within the black circle are below or slightly higher than 0, most of the area is classified as stratiform type. For this moment, threshold -0.5 shows better performance than 0.

Figure 6 shows the classification results from SVM, BAL^0, BAL$^{-0.5}$ (0801 UTC) and MRMS (0800 UTC) on 14 June 2012. In this case, MRMS, SVM, BAL^0 show similar performance in general, but BAL$^{-0.5}$ shows visible over classification of convective cells. The R^{CS} from MRMS, SVM, and BAL^0 show similar values around 22%, but BAL$^{-0.5}$ classifies much more pixels as connective with R^{CS} reaches 41% (Figure 6). Radar variables are shown in Figure 7, and a circle is also inserted in both Figures 6 and 7 to emphasize the performance from each approach in this circle. Inside the circle, the echoes with the Z values around 30∼35 dBZ have the chances to be either stratiform or convective type. On the other hand, the Z_{DR} shows low value around 0 dB, which is generally considered as the indicator of stratiform. It should be noted, it is impossible to show all the comparison results (every 5 minutes) as Figures 4∼7 from these two cases. Therefore, the results are shown in Figure 3 and Table 1 to quantitatively demonstrate their performance.

3.2.2 Tropical convective

Typhoon Morakot (6∼10 August 2009) brought significant rainfall to Taiwan. Over 700 people were reported dead in the storm, and the property loss was more than 3.3 billion USD. For most of the time during its landfall in Taiwan, the precipitation was classified as a mixture of tropical convective and tropical stratiform types. The performances of SVM, BAL^0, and BAL$^{-0.5}$ were validated with 96-hour data from 6 to 9 August 2009, where the results from 10 August 2009 were not included in the evaluation because no significant precipitation was observed. The time series plots of R^{CS}, shown in Figure 8, demonstrate that the R^{CS} from the BAL based approaches is evidently lower than the results from SVM and MRMS, and the latter two show similar performance during this 4-day period.

https://doi.org/10.5194/amt-2019-324
Preprint. Discussion started: 18 December 2019

Atmospheric Measurement Techniques Discussions

Classification results from BAL^0, $BAL^{-0.5}$, SVM (0402 UTC), and MRMS (0400 UTC) from 9 August 2009 are shown in Figure 9a, 9b, 9c, and 9d, respectively. The classification results in those regions, highlighted with two circles, are convective (SVM and MRMS) and stratiform (BAL^0 and $BAL^{-0.5}$). Figure 10 includes the reflectivity (10a), differential reflectivity (10b), and separation index (10c) from 0402 UTC, where the reflectivity field within the red rectangular box is shown in Figure 10d for more details. It was found that the heavy precipitation band is on the top of RCMK (Figure 10d), and this may cause significant attenuation and differential attenuation on Z and Z_{DR} fields. Although both Z and Z_{DR} fields were corrected, deficient or over compensations on Z and Z_{DR} fields lead to increased uncertainty on the separation index. It may be the primary reason causing the small values of the separation index. In Figure 10c, the separation index i are equal or less than -0.5 in the circled areas, and the BAL based approaches classify these regions as stratiform. On the other hand, these regions clearly show the convective precipitation features in the fields of Z (10a) and Z_{DR} (10b).

3.2.3 Stratiform precipitation event

The performances of BAL^0, $BAL^{-0.5}$, and SVM approaches were also evaluated with a widespread stratiform precipitation event on 26 March 2011. There were no convective type precipitations identified by MRMS, and all these three approaches showed consistent classification results with the MRMS result during 8-hour period evaluation.

4 Conclusions

A novel precipitation classification approach using support vector machine approach was developed and tested on a C-band polarimetric radar located in Taiwan. Different from other classification algorithms that use whole volume scan data, the proposed method only utilizes the data from the lowest unblocked tilt to separate precipitation into convective or stratiform type. It can be applied on new scanning schemes with more frequent scans at the lowest tilts and lack of information from a higher tilt, such as AVSET, SAILS, MRLE, and etc. Three radar variables of reflectivity, differential reflectivity, and the separation index derived by Bringi et al. (2009) are utilized in the new proposed approach, where both reflectivity and differential reflectivity need be corrected from attenuation and differential attenuation. Although the separation index alone can be used in the precipitation classification, there may be two potential limitations: thresholds and attenuation. Although the threshold "0" is proposed to separate convective from stratiform types, it was found that a single threshold may not sufficient for all cases. Other thresholds (such as"-0.5" used in the current work), sometimes can produce better results than "0". The attenuation is the other potential issue. Although both reflectivity and differential reflectivity should be corrected from attenuation before used in the separation index calculation, the correction biases on either filed may cause large uncertainty in the derived separation index and further lead to a wrong classification. This work attempts to propose a complementary method to enhance the performance of using separation index only. The proposed approach integrates input variables with a support vector machine method. The weighs and bias vectors used in the support vector machine were trained with typical stratiform and convective precipitation events. It should be noted that the proposed approach has a flexible framework, and some other variables can be easily included. With newly added variables, the weighting and bias vectors need to be retrained. The proposed approach was tested with multiple

https://doi.org/10.5194/amt-2019-324
Preprint. Discussion started: 18 December 2019

Atmospheric Measurement Techniques Discussions

cases, and its performance was found similar to a well-developed approach, MRMS, which utilizes multiple tilts radar data in the classification. It should be noted that the time difference between RCMK (i.e., BAL^{0} , $\mathrm{BAL}^{-0.5}$ and SVM) and MRMS could be as large as 5 minutes. Therefore, the pixel-to-pixel evaluation criteria of the probability of detection (POD) and false alarm rate (FAR) is not feasible for the evaluation. Although a new variable of R^{CS} is used in the performance evaluation, this should be treated as qualitative evaluation.

There are some issues need be noticed before applying this approach into operation. First, this approach is developed for fast scanning and fast update purpose, therefore, only the lowest tilt data is used as the input. With the higher tilt data as the inputs, potential enhancements should be expected. Second, the performance of the proposed approach depends highly on the training data, which should be selected very carefully. Third, coefficients in the separation index calculation depends on the local drop size distribution and drop shape relation features. Therefore, new relations need to be derived for the optimal results. Four, this work only presents a prototype algorithm. Given the flexible framework, other variables (such as differential phase) could be easily integrated into this algorithm, and the performance could be further enhanced.

Code and data availability.

The datasets and source code used in this study are available from the corresponding author upon request (yadwang@siue.edu).

Author contributions.

The algorithm was originally developed by Dr. Y. Wang. Dr. L. Tang processed the radar data including generate results from MRMS. Dr. P.-L. Chang and Miss Y.-S. Tang provided and processed radar data from CWB, they were further involved in algorithm discussion and article writing.

Competing interests.

The authors declare that there is no conflict of interest.

Acknowledgements. The authors thank the radar engineers from CWB help us collect and processing the radar data.

https://doi.org/10.5194/amt-2019-324
Preprint. Discussion started: 18 December 2019

Atmospheric Measurement Techniques Discussions

References

Adler, R. F. and Negri, A. J.: A satellite infrared technique to estimate tropical convective and stratiform rainfall, J. Appl. Meteor., 27, 30–51, 1988.

Anagnostou, E. N.: Doppler radar characteristics of precipitation at vertical incidence, Rev. Geophys. Space Phys., 11, 1–35, 2004.

Biggerstaff, M. I. and Listemaa, S. A.: An improved scheme for convective/stratiform echo classification using radar reflectivity, J. Appl. Meteor., 39, 2129–2150, 2000.

Bringi, V. N., Chandrasekar, V., Hubbert, J., Gorgucci, E., Randeu, W. L., and Schoenhuber, M.: Raindrop size distribution in different climatic regimes from disdrometer and dual-polarized radar analysis, J. Atmos. Sci., 60, 354–365–2122, 2003.

Bringi, V. N., Williams, C. R., Thurai, M., and May, P. T.: Using dual-polarized radar and dual-frequency profiler for DSD characterization: a case study from Darwin, Australial, J. Atmos. Oceanic Technol., 26, 2107–2122, 2009.

Burges, C. J. C.: A tutorial on support vector machines for pattern recognition, Data Min. Knowl. Discovery, 2, 955–974, 1998.

Carey, L. D., Rutledge, S. A., Ahijevych, D. A., and Keenan, T. D.: Correcting propagation effects in C-band polarimetric radar observations of tropical convection using differential propagation phase, J. Appl. Meteor., 39, 1405–1433, 2000.

Chang, W.-Y., Wang, T.-C. C., and Lin, P.-L.: Characteristics of the raindrop size distribution and drop shape relation in typhoon systems in the western Pacific from the 2D video disdrometer and NCU C-band polarimetric radar., J. Atmos. Oceanic Technol., 26, 1973–1993, 2009.

Gourley, J. J., Flaming, Z. L., Vergara, H., Kirstetter, P.-E., Clark, R. A., Argyle, E., Arthur, A., Martinaitis, S., Terti, G., Erlingis, J. M., Hong, Y., and Howard, K.: The FLASH project: improving the tools for flash flood monitoring and prediction across the United States, Bull. Amer. Meteor. Soc., 94, 799–805, 2016.

Grecu, M., Olson, W. S., Munchak, S. J., Ringerud, S., Liao, L., Haddad, Z. S., Kelley, B. L., and McLaughlin, S. F.: The GPM combined algorithm, J. Atmos. Oceanic Technol., 33, 2225–2245, 2016.

Haykin, S. O., ed.: Neural networks and learning machines, Pearson Higher Ed., PP 936, 2011.

Hong, Y., Kummerov, C. D., and Olson, W. S.: Separation of convective and stratiform precipitation using microwave brightness temperature, J. Appl. Meteor., 38, 1195–1213, 1999.

Houghton, H. G.: On precipitation mechanisms and their artificial modification, J. Appl. Meteor., 7, 851–859, 1968.

Houze, R. A. J., ed.: Cloud Dynamics, Academic Press, PP. 573, San Diego, 1993.

Houze, R. L.: Stratiform precipitation in regions of convection: A meteorological paradox?, Bull. Amer. Meteor. Soc., 78, 2179–2196, 1997.

Jameson, A. R.: The effect of temperature on attenuation correction schemes in rain using polarization propagation differential phase shift, J. Appl. Meteor., 31, 1106–1118, 1992.

Leary, C. A. and Jr., R. A. H.: Melting and evaporation of hydrometeors in precipitation from the anvil clouds of deep tropical convection, J. Atmos. Sci., 36, 669–679, 1979.

Park, S. G., Maki, M., Iwanami, K., Bringi, V. N., and Chandrasekar, V.: Correction of radar reflectivity and differential reflectivity for rain attenuation at X-band. part II: evaluation and application, J. Atmos. Oceanic Technol., 22, 1633–1655, 2005.

Penide, G., Protat, A., Kumar, V. V., and May, P. T.: Comparison of two convective/stratiform precipitation classification techniques: radar reflectivity texture versus drop size distribution-based approach, J. Atmos. Oceanic Technol., 30, 2788–2797, 2013.

Powell, S. W., Jr., R. A. H., and Brodzik, S. R.: Rainfall-type categorization of radar echoes using polar coordinate reflectivity data, J. Atmos. Oceanic Technol., 33, 523–538, 2016.

https://doi.org/10.5194/amt-2019-324
Preprint. Discussion started: 18 December 2019

Atmospheric Measurement Techniques Discussions

Ryzhkov, A. V. and Zrnic, D. S., eds.: Radar Polarimetry For Weather Observations, Springer Atmospheric Sciences, PP 477, 2019.

Skofronick-Jackson, G. and Coauthors: The global precipitation measurement GPM mission for science and society, Bull. Amer. Meteor. Soc., 98, 1679–1695, 2017.

Smith, T. M., Lakshmanan, V., Stumpf, G. J., Ortega, K. L., Hondl, K., Cooper, K., Calhoun, K. M., Kingfield, D. M., Manross, K. L., Toomey, R., and Brogden, J.: Multi-Radar Multi-Sensor (MRMS) severe weather and aviation products: Initial operating capabilities, Bull. Amer. Meteor. Soc., 97, 1617–1630, 2016.

Steiner, M. and Houze, R. A. J.: Three-dimensional validation at TRMM ground truth sites: Some early results from Darwin, Australia, 26^{th} Int.Conf. on Radar Meteorology, Norman, OK, Amer. Meteor. Soc., pp. 417–420, 1993.

Steiner, M., Jr., R. A. H., and Yuter, S. E.: Climatological characterization of three-dimensional storm structure from operational radar and rain gauge data, J. Appl. Meteor., 34, 1978–2007, 1995.

Testud, J., Bouar, E. L., Obligis, E., and Ali-Mehenni, M.: The rain profiling algorithm applied to polarimetric weather radar, J. Atmos. Oceanic Technol., 17, 332–356, 2000.

Thompson, E. J., Rutledge, S. A., Dolan, B., and Thursai, M.: Drop size distributions and radar observations of convective and stratiform over the equatorial Indian and West Pacific Oceans, J. Atmos. Sci., 72, 4091–4125, 2015.

Tokay, A. and Short, D. A.: Evidence from tropical raindrop spectra of the origin of rain from stratiform versus convective clouds, J. Appl. Meteor., 35, 355–371–4125, 1996.

Vulpiani, G., Montopoli, M., Passeri, L. D., Gioia, A. G., Giordano, P., and marzano, F. S.: On the use of dual-polarized C-band radar for operational rainfall retrieval in mountainous areas, J. Appl. Meteor. Climatol., 51, 405–425, 2012.

Wang, Y., Zhang, J., Ryzhkov, A. V., and Tang, L.: C-band polarimetric radar QPE based on specific differential propagation phase for extreme typhoon rainfall, J. Atmos. Oceanic Technol., 30, 1354–1370, 2013.

Wang, Y., Zhang, P., Ryzhkov, A. V., Zhang, J., and Chang, P.-L.: Utilization of specific attenuation for tropical rainfall estimation in complex terrain, J. of Hydrometeorology, 15, 2250–2266, 2014.

Yang, Y., Chen, X., and Qi, Y.: Classification of convective/stratiform echoes in radar reflectivity observations using a fuzzy logic algorithm, J. Geophys. Res. Atmos., 118, 1896–1905, 2013.

Zhang, G., ed.: Weather Radar Polarimetry, CRC Press PP 304, 2016.

Zhang, J., Howard, K., Langston, C., Vasiloff, S., Kaney, B., Arthur, A., Cooten, S. V., Kitzmiller, K. K. D., Ding, F., Seo, D.-J., Wells, E., and Dempsey, C.: National mosaic and multi-sensor QPE (NMQ) system: Description, results, and future plans, Bull. Amer. Meteor. Soc., 92, 1321–1338, 2011.

Zhang, J., Howard, K., Langston, C., Kaney, B., Qi, Y., Tang, L., Grams, H., Wang, Y., Cocks, S., Martinaitis, S., Arthur, A., Cooper, K., Brogden, J., and Kitzmiller, D.: Multi-Radar Multi-Sensor (MRMS) quantitative precipitation estimation: initial operating capabilities, Bull. Amer. Meteor. Soc., 97, 621–638, 2016.

https://doi.org/10.5194/amt-2019-324
Preprint. Discussion started: 18 December 2019

Atmospheric Measurement Techniques Discussions

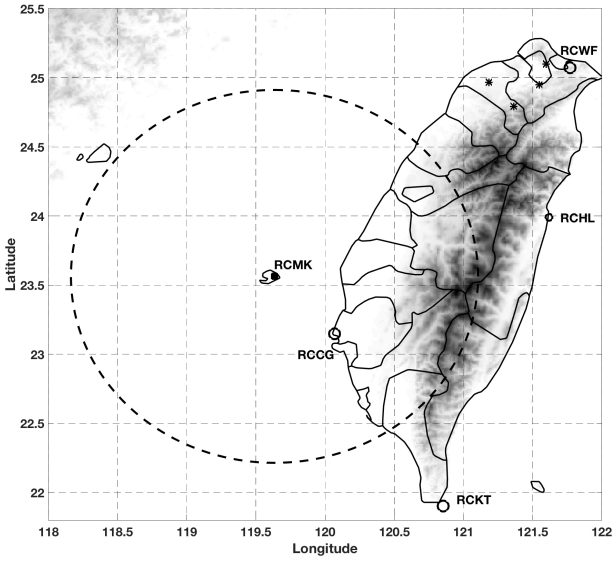

Figure 1. The terrain of Taiwan, the location of a C-band polarimetric radar RCMK (marked with a black square), JWDs (marked with black stars), and four S-band single polarization radar RCCG, RCKT, RCHL, and RCWF (marked with black circles).

https://doi.org/10.5194/amt-2019-324
Preprint. Discussion started: 18 December 2019

Atmospheric Measurement Techniques Discussions

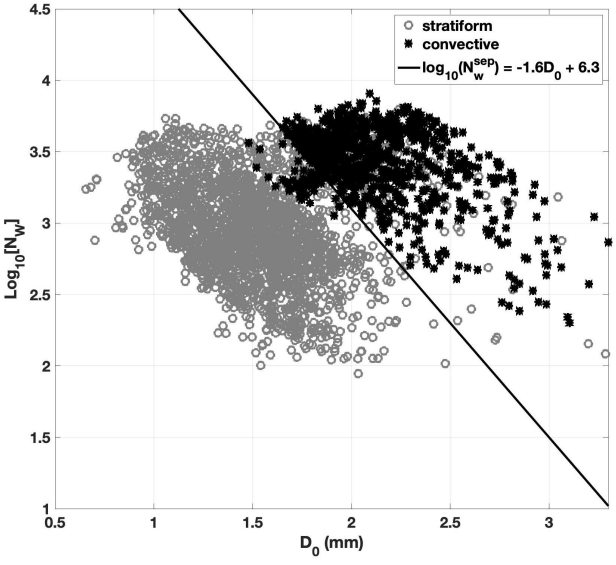

Figure 2. The distribution of $log10(N_w)$ vs D_0. The DSD data from stratiform and convective precipitations are presented with gray circles and black stars, and the separator line is shown with a solid line.

https://doi.org/10.5194/amt-2019-324
Preprint. Discussion started: 18 December 2019

Atmospheric Measurement Techniques Discussions

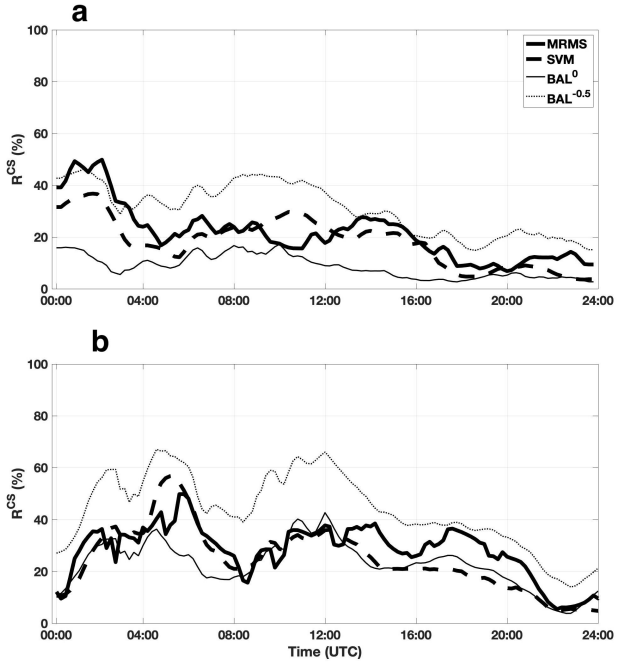

Figure 3. The time series plot of convective cells to stratiform cells ratio (R^{CS}) from 30 August 2011 (A) and 14 June 2012 (B). 24-hours data 0000 UTC 2400 UTC are used in each case. The results from BAL with threshold T_0 = -0.5, BAL with threshold T_0 = 0, SVM, and MRMS are indicated with thin dashed, thin solid, thick dashed and thick solid lines, respectively.

https://doi.org/10.5194/amt-2019-324
Preprint. Discussion started: 18 December 2019

Atmospheric Measurement Techniques Discussions

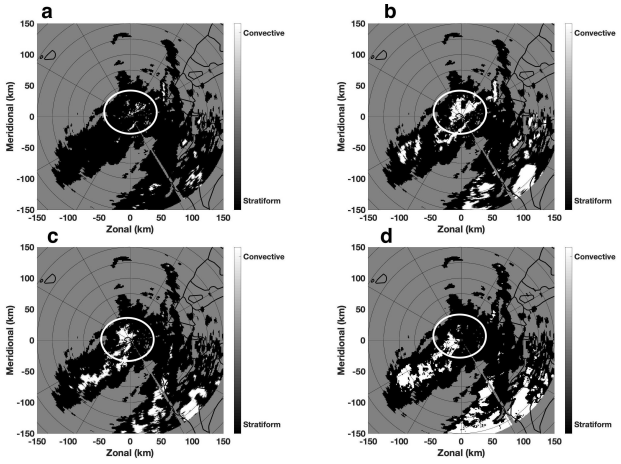

Figure 4. The classification results from BAL^{0} (a), BAL$^{-0.5}$(b), SVM (c) and MRMS (d). The time stamp for BAL^{0}, BAL$^{-0.5}$, and SVM is 0303 UTC 30 August 2011, and time stamp for MRMS is 0300 UTC 30 August 2011.

https://doi.org/10.5194/amt-2019-324
Preprint. Discussion started: 18 December 2019

Atmospheric Measurement Techniques Discussions

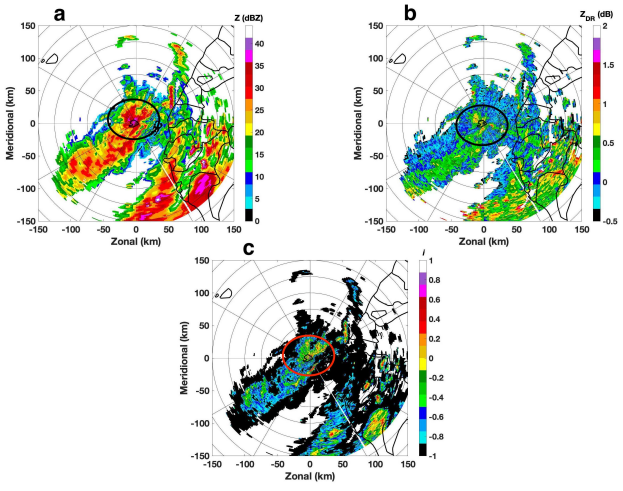

Figure 5. Radar variables of reflectivity (a), differential reflectivity (b), and separation index (c). The radar data was collected by RCMK at 0303 UTC 30 August 2011.

https://doi.org/10.5194/amt-2019-324
Preprint. Discussion started: 18 December 2019

Atmospheric Measurement Techniques Discussions

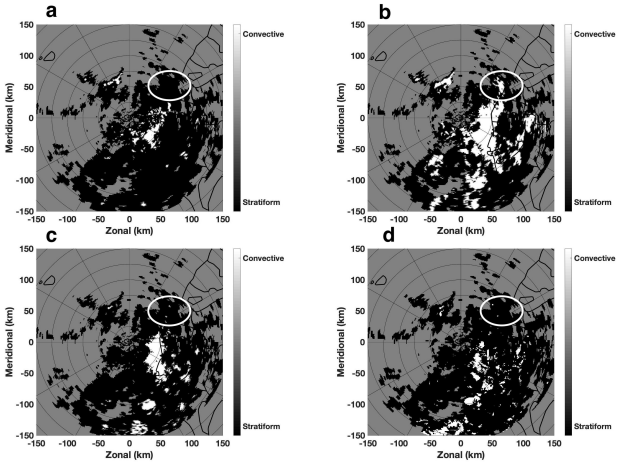

Figure 6. Similar to Figure 4 The results are from 14 June 2012. The time stamp for BAL^{0}, $BAL^{-0.5}$, and SVM is 0801 UTC, and time stamp for MRMS is 0800 UTC.

https://doi.org/10.5194/amt-2019-324
Preprint. Discussion started: 18 December 2019

Atmospheric Measurement Techniques Discussions

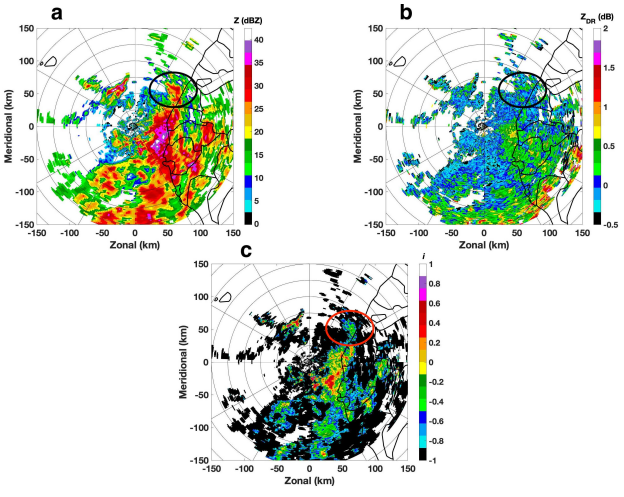

Figure 7. Similar to Figure 5, but radar data from 0801 UTC 14 June 2012.

https://doi.org/10.5194/amt-2019-324
Preprint. Discussion started: 18 December 2019

Atmospheric Measurement Techniques Discussions

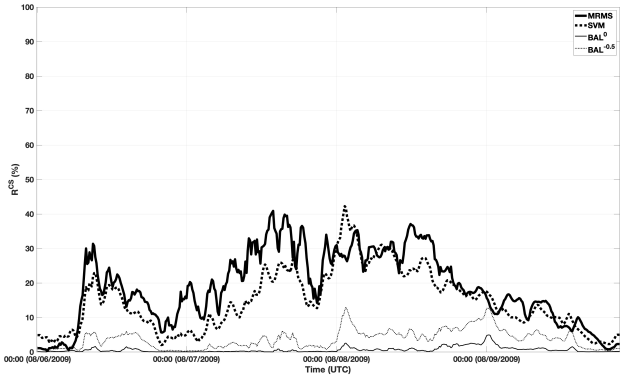

Figure 8. The time series plot of convective cells to stratiform cells ratio (R^{CS}) from 06 09 August 2009. 96-hours data are used in each case. The results from BAL with threshold T_0 = -0.5, BAL with threshold T_0 = 0, SVM, and MRMS are indicated with thin dashed, thin solid, thick dashed and thick solid lines, respectively.

https://doi.org/10.5194/amt-2019-324
Preprint. Discussion started: 18 December 2019

Atmospheric Measurement Techniques Discussions

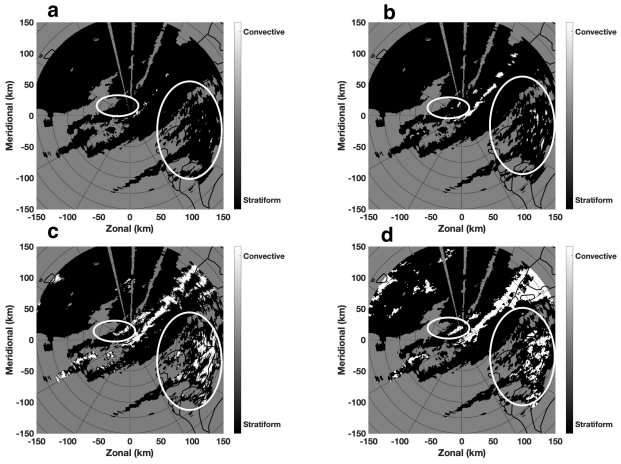

Figure 9. The classification results from BAL^{0} (a), BAL$^{-0.5}$(b), SVM (c) and MRMS (d). The time stamp for BAL^{0}, BAL$^{-0.5}$, and SVM is 0402 UTC 9 August 2009, and time stamp for MRMS is 0400 UTC 9 August 2009.

https://doi.org/10.5194/amt-2019-324
Preprint. Discussion started: 18 December 2019

Atmospheric Measurement Techniques Discussions

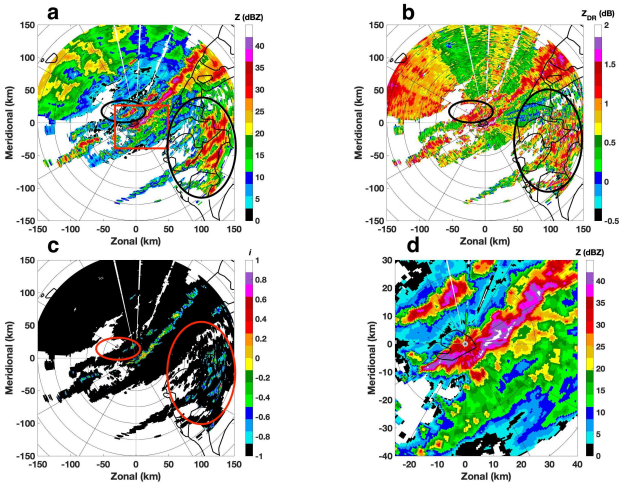

Figure 10. Radar variables of reflectivity (a), differential reflectivity (b), separation index (c), and reflectivity within the red rectangular box in A (d). The radar data was collected by RCMK at 0402 UTC 9 August 2009.

https://doi.org/10.5194/amt-2019-324
Preprint. Discussion started: 18 December 2019

Atmospheric Measurement Techniques Discussions

Table 1. The overall performance of these four precipitation events.

R^{CS} scores				
Case	BAL^{0}	BAL$^{-0.5}$	SVM	MRMS
30 August 2011	8%	30%	19%	21%
14 June 2012	15%	34%	18%	20%
06∼09 August 2009	1%	4%	17%	22%
26 March 2011	0%	0%	0%	0%
Total	4.3%	12.6%	16.6%	20.4%